THE ASTROPHYSICAL JOURNAL, 309:619–627, 1986 October 15

THE LYNDS 204 COMPLEX: MAGNETIC FIELD CONTROLLED EVOLUTION?

W. H. MCCUTCHEON
Department of Physics, University of British Columbia
F. J. VRBA
US Naval Observatory, Flagstaff
AND
R. L. DICKMAN AND D. P. CLEMENS[1, 2]
Five College Radio Astronomy Observatory and Department of Physics and Astronomy, University of Massachusetts
Received 1986 January 15; accepted 1986 April 2

ABSTRACT

The L204 dark cloud complex is a highly elongated structure stretching over 4° in declination. Its total mass is 400 $M_\odot$, with the more tenuous sections of the cloud being displaced in right ascension from the more heavily obscured parts.

We have observed $J = 1$–0 and 2–1 ^{12}CO and ^{13}CO emission over the complex and have also made optical polarization measurements of background stars along the length of the cloud. The CO radial velocities exhibit gradients along the length of the complex which mimic the variations in the mass distribution, and the polarization $\boldsymbol{E}$ vectors suggest that L204 contains a magnetic field predominantly perpendicular to its long dimension (assuming that the Davis-Greenstein mechanism is operative). These observations suggest that some external impulse acted on the complex over a large angular extent and that the subsequent evolution of the cloud has been controlled to a considerable extent by a magnetic field. Assuming virial equilibrium, we estimate an approximate value for the magnetic field in L204 to be ~ 50 μG.

Subject headings: interstellar: magnetic fields — nebulae: individual — polarization

I. INTRODUCTION

The star formation rate in molecular clouds is significantly smaller than would be predicted if all cloud material in the Milky Way were gravitationally collapsing (e.g., Zuckerman and Palmer 1974). Since thermal pressure is almost always too weak to significantly oppose the gravitational force in clouds of even modest densities, mechanisms such as turbulence, rotation, or magnetic fields are frequently invoked as possible retarding agents. The latter two stress mechanisms are intrinsically anisotropic, and in sufficiently simple systems—such as dark clouds undisturbed by massive star formation—cloud morphology might be expected to offer clues concerning which forces are inhibiting gravitational infall. Since the simplest interstellar magnetic field configuration—an infinitely long array of uniformly spaced flux lines—will, at sufficiently high magnetic intensities, permit collapse only in the single dimension along the field, the structure and evolution of filamentary dark clouds are of special interest in this connection. Such clouds are fairly common in the solar neighborhood (Schneider and Elmegreen 1981).

The simplest case of gravitational collapse in the presence of a magnetic field will produce an object compressed along its field lines with its long axis perpendicular to the field lines (Mestel 1965; Langer 1978). The standard Davis-Greenstein (1951) mechanism will align dust particles in the cloud and cause transmitted light to be polarized with its $\boldsymbol{E}$-vector parallel to the ambient $\boldsymbol{B}$-field. By measuring the linear polarization of stars near the edges of a number of nearby filamentary clouds, Vrba (1976), and Vrba, Strom, and Strom (1976) were able to determine the presence and orientations of magnetic fields in these objects. Curiously, in only one instance, was the simple collapse configuration, above, found to occur.

The Lynds 204 dark cloud complex (Lynds 1962) is a nearby example of an elongated filamentary structure which stretches over 4° in declination. It is considerably less massive than the objects originally studied by Vrba, Strom, and Strom, and because it appears free of contemporary star formation capable of perturbing the relationship between cloud and field morphology, it is a promising subject for detailed study. In this paper, we present the results of a broad observational program for this object, consisting of the following:

1) star counts over a large area from the Palomar Observatory Sky Survey (POSS) prints, used to determine the mass of the complex;

2) observations of λ 1.3 mm and 2.6 mm CO line emission from the common and ^{13}C-substituted forms; these provide a dynamical portrait of the L204 complex, as well as an independent mass tracer;

3) optical polarization measurements of some 60 background stars at the cloud edge, which permit us to infer the presence of a magnetic field within the cloud, and to determine its spatial orientation.

Taken together, the data reveal a complex whose morphology appears to be closely influenced by an internal magnetic field. The data also reveal an unprecedented correlation between the cloud's physical structure and its velocity field. We investigate some evolutionary ramifications of these facts.

II. OBSERVATIONS AND DATA ANALYSIS

a) Star Counts

Lynds 204 ($\alpha_0(1950) = 16^h45^m00.0^s$, $\delta_0(1950) = -12°00'00''$) is the central object in a 4° long dark cloud complex in Ophiuchus. The main body of the complex, which is composed

[1] Also Steward Observatory, University of Arizona.
[2] Bart J. Bok Fellow, 1985–1986.

of several clouds cataloged by Lynds, has also been designated Cloud 5 by Heiles and Katz (1976) and Globular Filament 3 by Schneider and Elmegreen (1981). Lynds estimated the visual extinction of the most opaque portions of the cloud to be at least 6 mag. As with most dark clouds, a distance assignment is not straightforward, but the position and radial velocity of the complex argue strongly for membership in the upper Scorpius cloud group (see Herbst and Warner 1981). For this study we assume the distance to be 170 pc.

Star counts were made from both red and blue POSS prints. The basic technique and associated uncertainties of the method are described in Dickman (1978*a*). Star counts were obtained for a reseau size of 2.'6 and where stars were present, extinctions determined from both prints were in reasonable agreement. For opaque regions, extinctions determined from the red prints alone were used. Counts were made at ~ 400 positions over the complex. Masses were determined within 10′ declination intervals using the formula given in Dickman (1978*a*) and a standard value for the gas to dust ratio (Jenkins and Savage 1978*a*) and a standard value for the gas to dust ratio (Jenkins and Savage 1974; Dickman 1978*b*). For areas of the cloud complex where stars were not counted, extinctions were estimated by interpolation. The total mass inferred over the declination range $-9°25' < \delta < -14°20'$ was $\sim 400\ M_\odot$.

b) Radio Line Data

Millimeter lines of ^{12}CO and ^{13}CO were observed between 1977 and 1984 on three different telescopes (see summary in Table 1). Since the large angular extent of the L204 complex prevented full mapping, observations were made at positions on a 5′ grid centered on the central coordinates listed above. Line intensities at all three facilities were calibrated using the standard ambient-temperature chopper technique (Penzias and Burrus 1973). Line strengths from the Aerospace telescope were subsequently converted to equivalent radiation temperatures by using the coupling efficiency for a uniformly filled main beam. Radio data from the other observatories were used solely for dynamical purposes, and line intensities were left as antenna temperatures.

As a check on the mass determined from star counts, an independent determination using LTE column densities of ^{13}CO and the conversion factor for molecular hydrogen column densities given by Dickman (1978*b*) was made. A value of 350 $M_\odot$ was obtained. Hereafter, we will assume the mass of the L204 complex to be 400 $M_\odot$.

c) Optical Polarization Measurements

Unfiltered, linear polarization measurements at optical wavelengths were obtained for 60 stars in the direction of L204.

TABLE 1

CO OBSERVATIONS

Telescope	Date	Isotope	Velocity Resolution (km s^{-1})	Beam Width
4.6 m Aerospace	1977	^{12}CO $J = 1$–0	0.65	2.'6
		^{13}CO $J = 1$–0	0.68	2.6
		C^{18}O $J = 1$–0	0.68	2.6
4.9 m MWO	1981	^{12}CO $J = 2$–1	0.08	1.3
		^{13}CO $J = 2$–1	0.09	1.3
14 m FCRAO	1984	^{12}CO $J = 1$–0	0.13	0.75
		^{12}CO $J = 2$–1	0.33	0.38

The observations were made with the Kinman photopolarimeter at the 4 m and 2.1 m telescopes of the Kitt Peak National Observatory (KPNO) and with the MINIPOL polarimeter at the 1.55 m telescope of the University of Arizona Observatories. The polarization results are presented in Table 2 with the coordinates of the observed stars measured from a glass copy of the POSS using the KPNO two-coordinate Grant measuring engine. The stellar positions are accurate to $\sim 1''$. Columns (4)–(6) give, respectively, the percentage polarization, the 1 σ standard deviation, and the position angle of the polarization.

III. RESULTS

a) Optical Polarization

Figure 1 displays the measured stellar polarization $\boldsymbol{E}$ vectors. Only measurements with $P/\sigma(P) > 2$ (corresponding to a position angle uncertainty of $< 15°$) are plotted. Figure 1 shows that the $\boldsymbol{E}$ vectors are generally orthogonal to the long axis of the cloud complex. The alignment of the polarization vectors with respect to the long axis in the southernmost cloud is somewhat different, being $\sim 30°$ from orthogonality. This southern cloud does not appear to be connected to the long complex above it and is assumed to be a separate object.

The simplest and most common explanation for large-scale polarizations in the Galaxy is the magnetic alignment of elongated dust grains (see, e.g., Aannestad and Purcell 1973). We assume that this mechanism is responsible for the coherent and fairly large polarizations observed along the main cloud filament in Figure 1. Two important questions must then be addressed. First, is the magnetic field responsible for the polarization in Figure 1 representative of the cloud? Second, what is the alignment of the observed $\boldsymbol{E}$ vectors with respect to the field?

Since the L204 cloud is presumed to be at the distance of the ρ Oph dark cloud complex ($d \approx 150$–170 pc) and is at relatively high galactic latitude ($b \approx +20°$), both foreground and background interstellar extinctions should be small. The average value for the extinction in the interstellar medium is 1.8 mag kpc^{-1} (Spitzer 1978). The value of A_v expected foreground to L204 then is ~ 0.3 mag, and the total value expected along the line of sight to the edge of the galactic gaseous disk at $b = +20°$ is ~ 0.6 mag, assuming an H I scale height of 125 pc. The stars selected for observations were generally chosen to lie toward regions of obvious optical opacity. For the stars in Table 2 with significant polarization [$P/\sigma(P) \geq 3$], the average value of A_v is 1.3 mag based on the star count analysis described in § II *a*. Thus, stars with significant polarization appear to suffer extinction due primarily to material in L204.

Figure 2 shows how the ratio of observed polarization, P, to extinction, A_v, varies with A_v for stars with a significant value of A_v (≥ 0.5 mag). Since there is some uncertainty in individual values of A_v, inherent in the star count method, individual values of P/A_v are, in some cases, apparently larger than the maximum average value $P/A = 3\%$ mag^{-1} (Vrba, Strom, and Strom 1976; Vrba, Coyne, and Tapia 1981; Serkowski, Mathewson, and Ford 1975). While this is an expected artifact of the large uncertainties in A_v, particularly at the lowest values of A_v where the percentage uncertainties are largest, it is nonetheless clear that P/A_v decreases at higher values of A_v. This would be expected if the same grains produce both polarization and extinction: net polarization cannot increase as fast as optical depth due to the depolarizing effects of dust

TABLE 2

UNFILTERED OPTICAL POLARIZATION MEASUREMENTS OF STARS NEAR LYNDS 204

Star Number (1)	α(1950) (2)	δ(1950) (3)	P(%) (4)	$\sigma(P)$ (5)	θ (6)
1.....	16 44 58.4	−09 28 29	1.28	0.36	92°
2.....	16 44 51.0	−09 31 03	3.34	0.82	88
3.....	16 45 10.7	−09 56 31	2.95	0.81	114
4.....	16 45 23.8	−09 58 39	0.85	0.48	98
5.....	16 45 49.0	−10 13 22	2.66	0.75	86
6.....	16 45 47.4	−10 23 09	1.68	0.45	83
7.....	16 46 09.2	−10 40 25	0.77	0.84	53
8.....	16 46 18.3	−10 44 40	2.2	1.6	52
9.....	16 46 14.8	−11 06 16	4.4	1.0	79
10.....	16 45 57.4	−11 08 01	2.48	0.71	78
11.....	16 45 53.7	−11 17 28	2.09	0.70	82
12.....	16 45 44.6	−11 34 58	2.77	0.50	79
13.....	16 45 20.6	−11 48 02	3.9	1.8	23
14.....	16 45 09.1	−12 04 41	3.7	1.3	99
15.....	16 45 03.6	−12 06 22	0.8	1.2	59
16.....	16 45 07.5	−12 13 38	1.19	0.31	91
17.....	16 45 04.5	−12 32 55	1.87	0.45	84
18.....	16 45 23.7	−12 43 53	0.50	0.21	122
19.....	16 45 52.3	−13 05 03	5.1	1.9	77
20.....	16 45 30.0	−13 25 40	0.45	0.42	99
21.....	16 45 34.3	−13 49 48	2.13	0.39	68
22.....	16 45 32.7	−13 56 28	2.50	0.41	62
23.....	16 45 27.0	−14 00 29	3.87	0.44	45
24.....	16 46 00.0	−13 59 58	2.91	0.47	54
25.....	16 46 04.2	−13 57 28	2.11	0.80	47
26.....	16 46 13.8	−13 54 48	3.38	0.70	61
27.....	16 46 37.7	−14 00 39	1.87	0.82	72
28.....	16 46 57.8	−14 02 45	5.34	0.89	62
29.....	16 47 42.4	−14 07 27	2.84	0.58	56
30.....	16 47 21.8	−14 10 42	2.66	0.17	24
31.....	16 46 11.0	−14 11 57	0.85	0.38	136
32.....	16 45 52.5	−14 19 59	2.07	0.84	80
33.....	16 45 47.7	−14 14 50	3.85	0.58	69
34.....	16 45 32.2	−14 05 27	0.27	0.76	162
35.....	16 45 20.0	−14 08 53	2.49	0.73	42
36.....	16 44 09.0	−13 49 18	2.72	0.93	58
37.....	16 44 34.0	−13 48 18	1.26	0.49	63
38.....	16 45 06.4	−13 47 10	4.86	0.55	58
39.....	16 44 51.5	−12 49 41	1.60	0.26	100
40.....	16 44 53.8	−12 45 10	0.90	0.17	128
41.....	16 44 26.5	−12 11 43	2.13	0.45	37
42.....	16 44 26.5	−12 08 10	2.68	0.56	39
43.....	16 44 24.0	−12 00 56	0.89	0.51	56
44.....	16 45 26.6	−11 38 27	2.60	0.80	61
45.....	16 45 33.8	−11 31 39	2.04	0.30	65
46.....	16 45 42.3	−11 26 09	1.52	0.30	73
47.....	16 45 49.1	−11 21 48	1.0	1.0	21
48.....	16 45 44.9	−11 11 41	2.94	0.60	78
49.....	16 45 09.2	−10 54 41	1.5	1.7	83
50.....	16 45 14.2	−10 06 31	4.09	0.36	107
51.....	16 44 22.8	−09 36 04	1.27	0.42	68
52.....	16 44 06.1	−09 34 09	2.9	1.2	79
53.....	16 43 31.9	−09 30 56	1.31	0.45	45
54.....	16 43 38.9	−09 28 39	2.16	0.25	64
55.....	16 44 19.0	−09 26 02	3.6	1.9	82
56.....	16 44 36.4	−09 25 10	5.5	3.4	18
57.....	16 44 26.9	−09 22 12	2.00	0.27	77
58[a].....	16 45 23.5	−13 23 17	0.88	0.39	10
59[a].....	16 45 17.0	−09 59 17	1.45	0.12	133
60[a].....	16 45 19.8	−10 00 49	1.80	0.07	101

[a] Stars with positional accuracies to ±5″ only.

grain collisions with the gas (Vrba, Coyne, and Tapia 1981). This behavior is, in fact, typical of dark clouds with densities greater than about 100 cm^{-3} (Vrba, Strom, and Strom 1976; Vrba, Coyne, and Tapia 1981; Vrba, Coyne, and Tapia 1986; Guetter and Vrba 1986; Vrba and Guetter 1986). The above discussion and Figure 2 are consistent with most of the polarization occurring in the dark cloud.

We shall assume the Davis-Greenstein grain alignment theory to be valid so that surviving polarization $\boldsymbol{E}$ vectors (i.e., the vectors indicated in Figure 1) are parallel to the magnetic field vector, $\boldsymbol{B}$ (see discussions by Greenberg 1968 and Chaisson and Vrba 1978). This situation occurs when the temperature inequality $T_{grain} < T_{gas}$ holds, and is likely to be true in the less dense regions of the cloud, and away from areas where there are embedded protostellar or young stellar sources. There is no evidence of either of these objects in the L204 complex. Additional support for the alignment of $\boldsymbol{E}$ parallel to $\boldsymbol{B}$ comes from the polarization studies of Hall (1958), Mathewson and Ford (1970), and Axon and Ellis (1976). Data from their measurements were used to produce Figure 3, which shows polarization vectors with magnitudes greater than 0.3% for stars closer than 1 kpc over a 1600 square degree field centered on the dark cloud complex. This figure shows how the L204 complex and its polarization lie with respect to the larger field in which it is embedded. The $\boldsymbol{E}$ vector directions in this figure are generally parallel to those shown in Figure 1. The conditions for the Davis-Greenstein mechanism to be operative in the general interstellar medium are almost certainly in effect, and one would not expect the field to change abruptly upon entering the outer portions of the denser complex.

In summary, our view is that the magnetic field of the cloud is part of the general galactic field, and with the exception of the southernmost cloud, lies primarily perpendicular to the long axis of the L204 complex.

b) CO Velocity Data

The CO line centroid velocities, plotted in Figure 4 as a function of declination, form a remarkable pattern which mimics the morphology of the cloud complex (see Fig. 4 and Table 1). Velocities obtained from 6 cm H_2CO observations by Heiles and Katz (1976), although much less extensive than our CO observations, also fit the pattern (but the pattern is not recognizable from those data alone). Since the two variables plotted as abscissae in Figure 4 are measured along orthogonal directions, this suggests that we are observing the projection of a true displacement lying between 0° and 90° with respect to the line of sight.

Figure 4 shows that the most tenuous, and hence least massive, sections of the complex have the smallest radial velocities (the pattern is most noticeable in the declination range $-80' < \Delta\delta < 80'$). This suggests that the complex as a whole possessed an initial velocity V_0 and that some external impulse has acted to give the least massive sections a velocity displacement. Figure 5 shows this result in another form. All radial velocities at a given declination have been averaged and plotted against declination in the left-hand panel. In the right-hand panel, the total mass of each 10′ long cloud segment is plotted against the declination of the segment center. There is a high correlation between the bumps in each plot, implying that the most massive sections of the L204 filament have the smallest velocity displacement from V_0. Although there are fewer data points, the southernmost section again behaves somewhat differently, with the mass-velocity correlation being weaker.

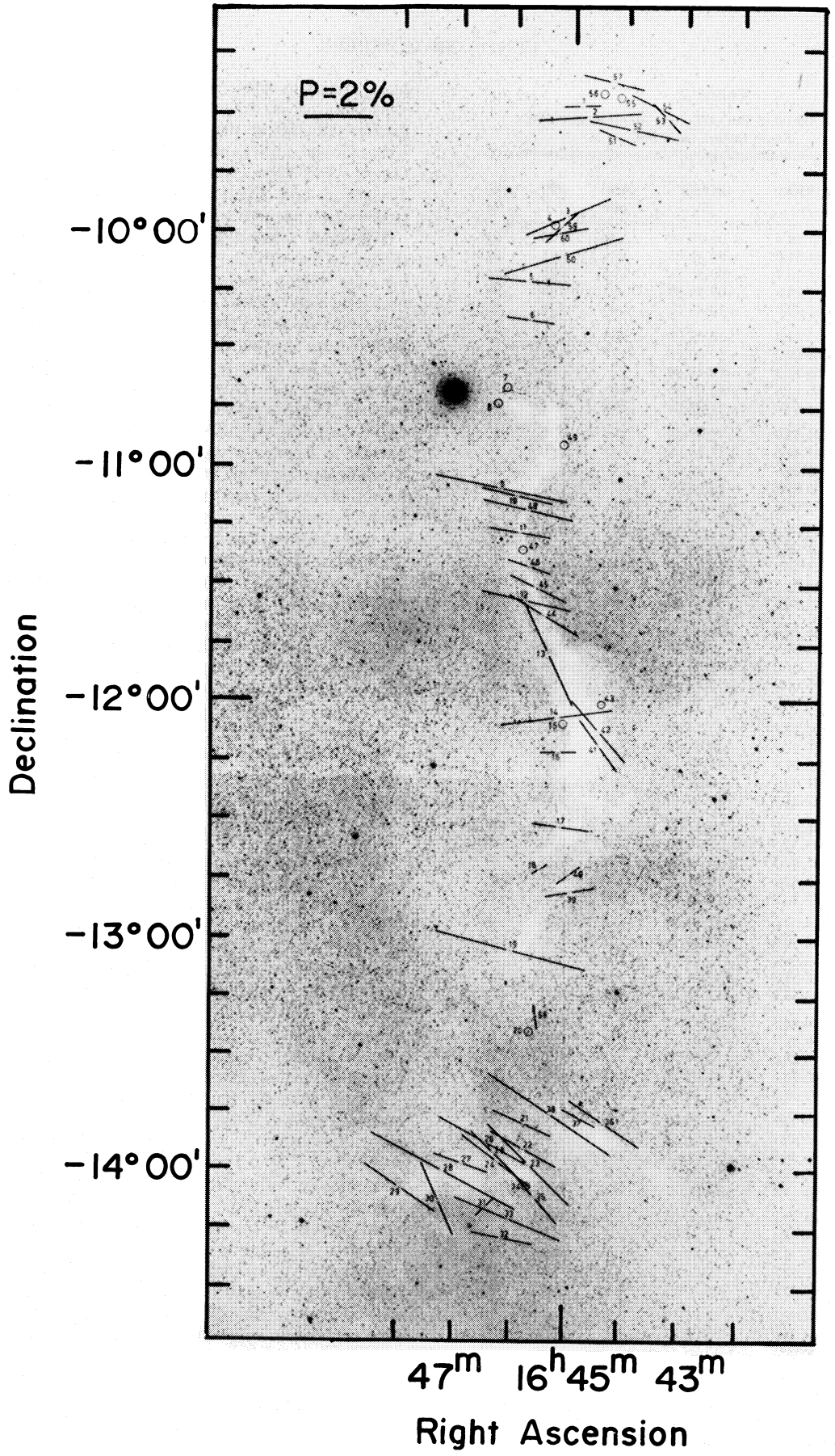

FIG. 1

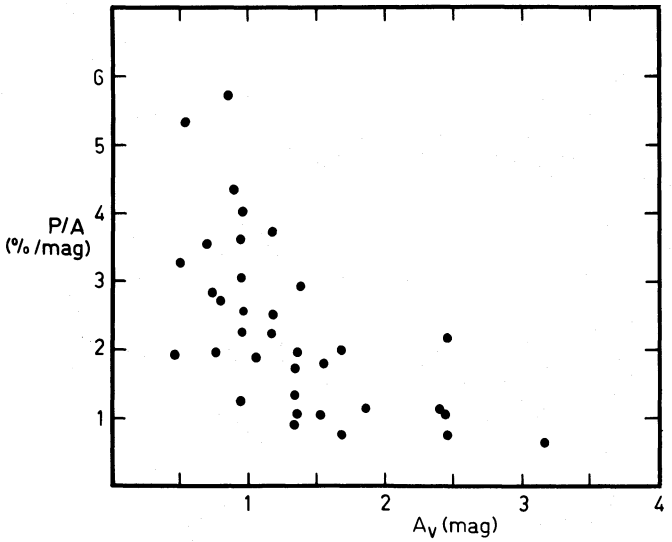

FIG. 2.—Ratio of polarization to visual extinction, vs. visual extinction (in magnitudes) for selected stars around the periphery of the L204 complex.

Taken together with the polarization data (§ III*a*), this leads us to suspect that this southern cloud is only weakly coupled to the main complex and perhaps is only partially controlled by the magnetic field (see § IV).

If the above scenario is correct, and if the momentum transferred to various sections of the cloud by an external impulse is constant, then $M_i(V_i - V_0) = \text{const}$, where M_i and V_i are the mass and velocity of the ith segment. The quantity V_0 will then be the vertical intercept in a plot V_i against $1/M_i$. Plots of this form were constructed for the declination offset ranges $75' \geq \Delta\delta \geq 15'$ and $5' \geq \Delta\delta \geq -65'$ where the visual correlations in Figure 4 are highest. The values determined for V_0 were 4.2 ± 0.6 km s^{-1} and 4.8 ± 0.3 km s^{-1}, respectively. The weighted mean gives $V_0 = 4.7$ km s^{-1}.

IV. DISCUSSION

The L204 complex is remarkable in two respects: (i) It exhibits a large-scale magnetic field alignment in a direction orthogonal to its long axis, which extends over a length of ~ 10 pc (Fig. 1). (ii) Its velocity structure in a declination-velocity plot is very similar to its morphological structure

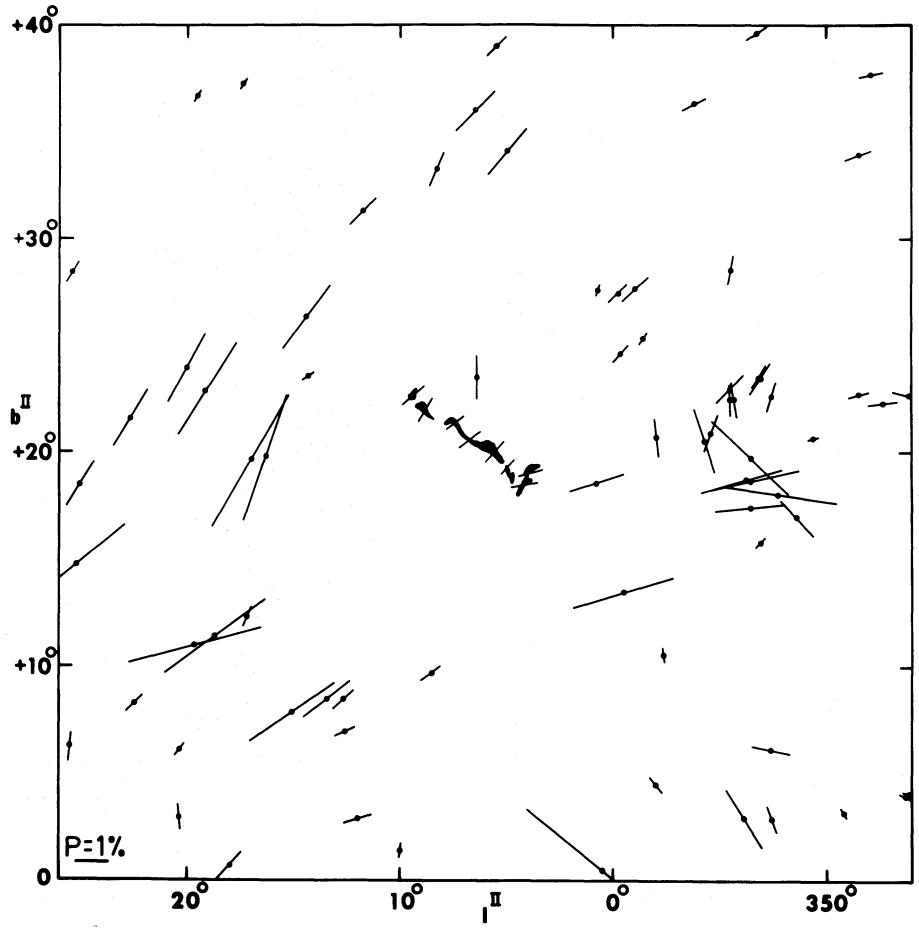

FIG. 3.—Polarization vectors with magnitudes greater than 0.3% for stars closer than 1 kpc over a 1600 square degree field centered on the complex. Data were obtained from Hall (1958), Mathewson and Ford (1970), and Axon and Ellis (1976). A few generic polarization vectors are plotted on the dark cloud complex.

FIG. 1.—Polarization vectors (magnitude and direction) for the stars indicated, drawn on a reproduction of the Palomar Sky Survey red print. The circles identify stars having values of the ratio $P/\sigma(P) < 2$.

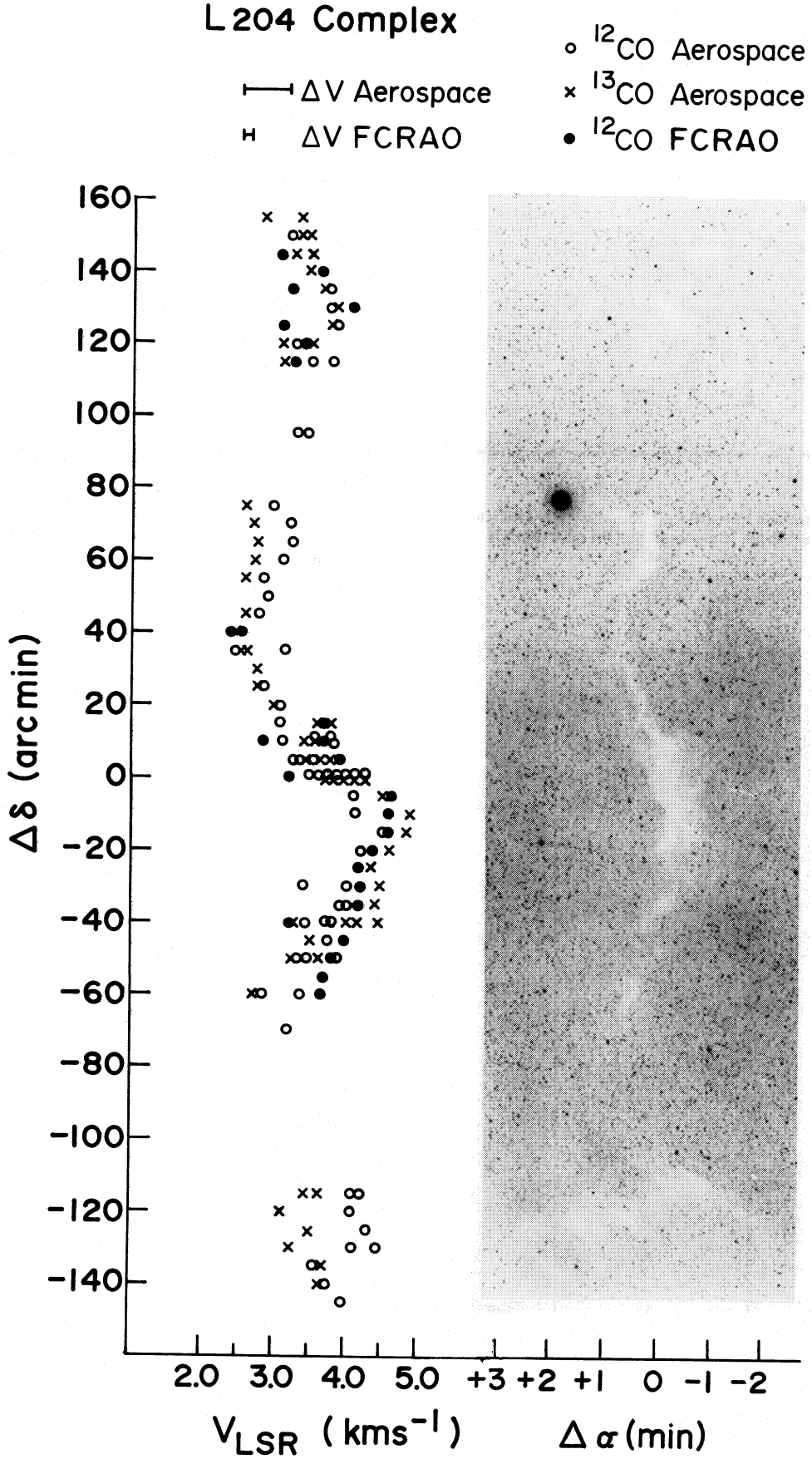

FIG. 4.—Declination offset vs. CO LSR velocities for the L204 complex, aligned in declination with a print of the complex reproduced from the Palomar Sky Survey red print. The central coordinate is $\alpha(1950) = 16^h45^m00^s$, $\delta(1950) = -12°00'00''$. For clarity, not all the CO velocities observed have been shown.

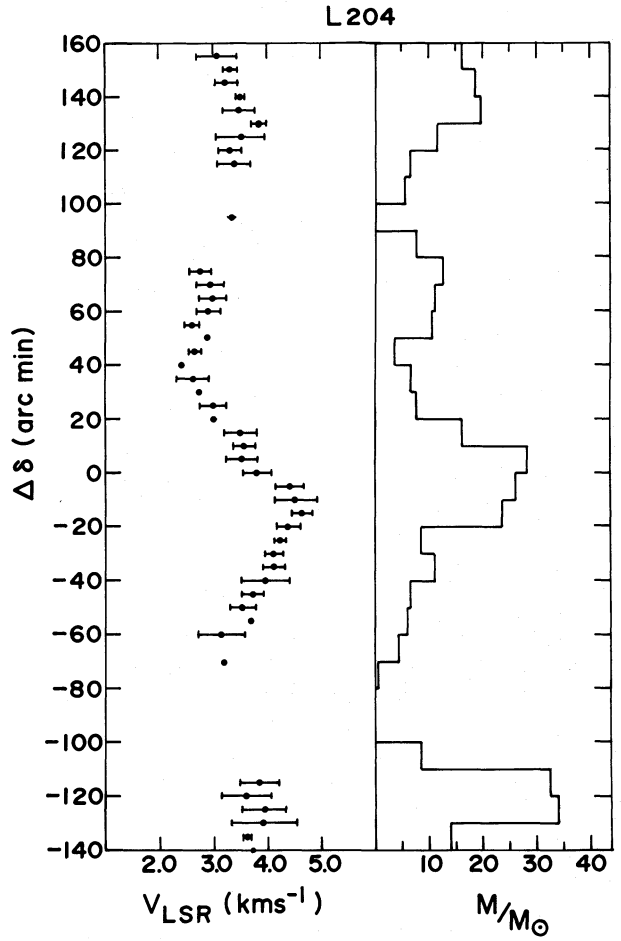

FIG. 5.—*Left panel:* The CO LSR velocities, averaged at each declination, as a function of declination. The error bars are the standard deviations of the mean velocities. *Right panel:* The mass of the complex in each 10′ declination interval as a function of declination. The panels are aligned in declination. The central declination is $\delta(1950) = -12°00'00''$.

(Fig. 4). Point (ii) implies that some external influence acted on the cloud over a large angular extent to displace the sections with smaller mass from those with large mass. With respect to (i), we have stated reasons why we believe that the measured *E* vectors run parallel to the magnetic field in the outer envelope of the cloud. To proceed further, we assume that the magnetic field extends well into the interior of the cloud. This seems reasonable since magnetic ion slip models require critical densities considerably larger than the value $\sim 10^3$ cm^{-3} which appears to be present in L204. A global magnetic field threading the cloud provides a natural structure for keeping the disturbance which acted on the cloud coherent.

While it is tempting to view L204 as a highly flattened complex which collapsed in one dimension along the field lines according to models described by Mestel (1965) and Langer (1978), this scenario does not appear to be applicable. Our velocity information shows that the cloud is moving at an angle less than 90° with respect to the line of sight, and we should then see a sheetlike geometry clearly if it were present. Our data suggest instead that the cloud is flattened in two dimensions. They also strongly suggest that the magnetic field is presently affecting the movement of the gas. If the complex is assumed to be in equilibrium the virial theorem may be used to estimate the magnetic field. Such a magnetically controlled cloud arises from the balance between the gravitational pressure and the sum of the kinetic and magnetic pressures.

Determination of the gravitational pressure (Ω/V, where Ω is the gravitational potential energy and V is the volume) requires a knowledge of the specific geometry of the cloud. Here we assume a cylindrical geometry as a rough approximation to the elongated, flattened, and nonuniform complex. For a uniform disk of radius a, and height $2h$, the gravitational potential energy is given by

$$\Omega = -\frac{1}{3}\frac{GM^2h}{a^2} \quad (1)$$

(Bowers and Deeming 1984). The gravitational pressure, $p_{\rm grav} = \Omega/V$, is independent of h, but is proportional to $1/a^4$. For $M = 400\ M_\odot$, and $a = 0.70$ pc, $p_{\rm grav} = 1.02 \times 10^{-10}$ dynes cm^{-2}. Assuming the CO linewidths to be due to turbulence, the kinetic pressure of the gas is given by

$$p_{\rm kin} = 2/3 n m_p v^2 , \quad (2)$$

where n is the density, m_p the proton mass, and v the velocity dispersion. For $n = 10^3$ cm^{-3}, and $v = 0.7$ km s^{-1}, $p_{\rm kin} = 5.4 \times 10^{-12}$ dynes cm^{-2}.

The magnetic pressure is given by

$$\frac{B^2}{8\pi} = p_{\rm grav} - p_{\rm kin}, \quad (3)$$

and this gives a value $B = 49$ μG. In reality, the complex is thinner at the top and bottom than in the middle, and if the radius were decreased by a factor of 2, B would increase by a factor of 4. This value of $B \approx 200$ μG is an upper limit. A value ≤ 50 μG is more appropriate since a thin sheet configuration, inclined to the line of sight and indistinguishable from a cylinder, would have a value of $P_{\rm grav}$ smaller than that calculated above, and hence B would be lower. Evidence that the cloud depth, along the line of sight, is somewhat greater than the width is suggested by CO emission and extinction values toward the edges. Here, where $A_v \approx 1$–2 mag, weak CO emission implies $n \approx 3 \times 10^2$ cm^{-3}. Using the standard gas-to-dust ratio (Jenkins and Savage 1974), the depth for these values is $\sim 10^{19}$ cm or ~ 3 pc.

A value for B of several tens of μG is consistent with expectations for the galactic magnetic field which has been amplified as the complex flattened. Theories of field amplification, expressed as $B \propto n^k$, give values of k lying in the range $\frac{1}{3} \leq k \leq \frac{1}{2}$ (Mouschovias 1976). Using the value $k \approx 0.4$ determined for the cloud R CrA by Vrba, Coyne, and Tapia (1981), one finds that for a density increase from 5 cm^{-3} to 10^3 cm^{-3}, and for an initial value of B equal to 5 μG, the final B will be ~ 40 μG.

While it therefore seems plausible that the present magnetic field strength in L204 was attained by compressional amplification of the ~ 5 μG galactic field, it also seems likely that the compression itself may have been externally initiated. Figure 4 strongly suggests that the complex as we now see it has been acted upon by an external impulse, and Figure 6 shows that the contours of CO emission on the western side of the central cloud are compressed significantly compared to those on the eastern side. We have calculated the time scales for displacements of the various sections to occur and these all lie in the range (1.0–3.0) $\times 10^5$ yr. While we have not been able to identify unambiguously the event that caused this displacement, and possibly the collapse of the complex from some larger

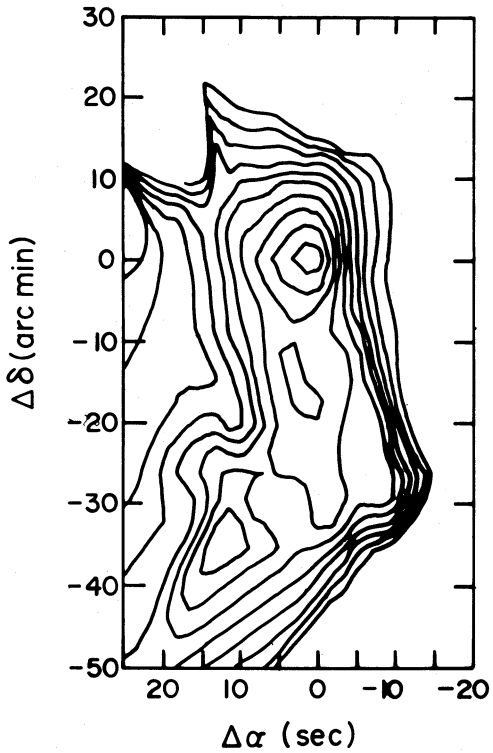

FIG. 6.—Integrated $J = 2$–1 CO emission contours for the central cloud in the velocity range 2–7 km s^{-1}. The central coordinate is the same as for Fig. 3.

configuration, an interesting possibility is the influence of ζ Oph. This O9 star is a runaway, with a possible origin in the Sco OB2 complex and an estimated kinematic age of $\sim 1.1 \times 10^6$ yr (Herbst and Warner 1981). Zeta Ophiuchus presently has a stellar wind with $\dot{M} \approx 10^{-7}\ M_\odot\ \mathrm{yr}^{-1}$ and $V \approx 1200$ km s^{-1} (D. Morton, personal communication). Over 10^6 yr, the total kinetic energy contained in the stellar wind $\sim 1.5 \times 10^{48}$ ergs. If the star were at a mean distance D from L204 for this period, the energy deposited on a cylindrical complex would be $\sim 1.5 \times 10^{48}(2ah)/(4\pi D^2)$ ergs, where a is the radius of the cylinder and h the length. The total translational kinetic energy in the complex, obtained by summing the energies for the various 10′ sections is $4.1 \times 10^{45}\ \sec^2 \Theta$ ergs, where Θ is the angle of the displacement velocity of the cloud with respect to the line of sight. Setting $a = 0.7$ pc and $h = 10$ pc as above and $\Theta = 45°$, we obtain $D = 14.3$ pc. For a complex which has a depth of ~ 3 pc as suggested earlier, $D \approx 21$ pc.

The distance to ζ Oph is 200 pc (Lesh 1968), only ~ 30 pc farther than the estimated distance to L204. This suggests that ζ Oph is too far from L204 to have had a major influence, particularly in view of our assumption of a perfectly efficient interaction between the stellar wind and the cloud, a highly unlikely situation. Even if the distances to L204 and ζ Oph are the same, the separation between the two would be ~ 8 pc, which is still too large for the stellar wind to be effective for a coupling efficiency which could be as low as a few percent.

However, if the L204 complex collapsed from a larger cloud and the present velocities are a continuation of the original motion, ζ Oph may have been even closer to the cloud in the past and might have been the driving agent for the present configuration. The compressed contours of CO emission (Fig. 6) on the estern side of L204, toward ζ Oph, are possibly tracing out the windward side of the cloud.

V. SUMMARY

Our main conclusions are as follows.

1. Linear polarization vectors of stars at the edges of the filamentary dark cloud Lynds 204 are aligned predominantly in a direction orthogonal to the long axis of the cloud. We conclude that this is also the direction of the ambient magnetic field. A plot of the polarization to extinction ratio against extinction gives strong evidence that the magnetic field is associated with the dark cloud complex.

2. A declination versus velocity of CO emission plot mimics the geometrical shape of the complex, with the least massive sections of the complex having the smallest radial velocity. This suggests that the complex as a whole was aligned in declination and acted upon by some external impulse. Compressed CO emission contours on the western side of the L204 cloud support this idea.

3. The large-scale velocity structure of the complex suggests that the external influence acted over a large angular extent. The magnetic field would have provided a natural structure for keeping an external disturbance coherent, possibly suggesting that the magnetic field is responsible for the cloud's present morphology. Assuming the cloud complex to be in hydrostatic equilibrium, the virial theorem yields an approximate value for the magnetic field of ~ 50 μG.

We are grateful to G. Coyne and S. Tapia for obtaining some of the polarization measurements, and to J. White for assistance with the Aerospace observations. F. J. V. is especially grateful to S. and K. Strom who suggested the polarization measurements and assisted in the observations. W. H. M. gratefully acknowledges grants in aid of research from the Natural Sciences and Engineering Research Council of Canada. Work by R. L. D. and D. P. C. was supported by National Science Foundation grant AST82-12252 to the Five College Radio Astronomy Observatory.

The Aerospace spectral line radio astronomy program was supported jointly by Natural Science Foundation grant MPS73-04554 and the Aerospace Corporate Program for Research and Investigation.

The Five College Radio Astronomy Observatory is operated with support from the National Science Foundation under grant AST-12252 and with permission of the Metropolitan District Commission, the Commonwealth of Massachusetts.

The Millimeter Wave Observatory is operated by the Electrical Engineering Research Laboratory of the University of Texas at Austin with support from the National Science Foundation and McDonald Observatory.

REFERENCES

Aannestad, Per., and Purcell, E. M. 1973, *Ann. Rev. Astr. Ap.*, **11**, 309.
Axon, D. J., and Ellis, R. S. 1976, *M.N.R.A.S.*, **177**, 499.
Bowers, R., and Deeming, T. 1984, *Astrophysics II* (Boston: Jones and Barlett).
Chaisson, E. J., and Vrba, F. J. 1978, in *Protostars and Planets*, ed. T. Gehrels (Tucson: University of Arizona Press), p. 189.
Davis, L., and Greenstein, J. L. 1951, *Ap. J.*, **114**, 206.
Dickman, R. L. 1978*a*, *A.J.*, **83**, 363.
———. 1978*b*, *Ap. J. Suppl.*, **37**, 407.
Greenberg, J. M. 1968, in *Nebulae and Interstellar Matter*, ed. B. Middlehurst and L. Aller (Chicago: University of Chicago Press), p. 221.
Guetter, H. H., and Vrba, F. J. 1986, in preparation.
Hall, J. S. 1958, *Pub. US Naval Obs.*, 2d Ser., Vol. **17**, No. V1.

Heiles, C., and Katz, G. 1976, *A.J.*, **81**, 37.
Herbst, W., and Warner, J. W. 1981, *A.J.*, **86**, 885.
Jenkins, E. B., and Savage, D. B. 1974, *Ap. J.*, **187**, 243.
Langer, W. D. 1978, *Ap. J.*, **255**, 95.
Lesh, J. R. 1968, *Ap. J. Suppl.*, **17**, 371.
Lynds, B. T. 1962, *Ap. J. Suppl.*, **7**, 1.
Mathewson, D. S., and Ford, V. L. 1970, *Mem. R.A.S.*, **74**, 139.
Mestel, L. 1965, *Quart. J.R.A.S.*, **6**, 265.
Mouschovias, T. 1976, *Ap. J.*, **207**, 141.
Penzias, A. A., and Burrus, C. A. 1973, *Ann. Rev. Astr. Ap.*, **11**, 51.
Schneider, S., and Elmegreen, B. G. 1981, *Ap. J. Suppl.*, **41**, 87.
Serkowski, K., Mathewson, D. S., and Ford, V. L. 1975, *Ap. J.*, **196**, 261.
Spitzer, L. 1978, *Physical Processes in the Interstellar Medium* (New York: Wiley).
Vrba, F. J. 1976, Ph.D. thesis, University of Arizona.
Vrba, F. J., Coyne, G. V., and Tapia, S. 1981, *Ap. J.*, **243**, 489.
———. 1986, in preparation.
Vrba, F. J., and Guetter, H. H. 1986, in preparation.
Vrba, F. J., Strom, S. E., and Strom, K. M. 1976, *A.J.*, **81**, 958.
Zuckerman, B., and Palmer, P. 1974, *Ann. Rev. Astr. Ap.*, **12**, 279.

D. P. CLEMENS: Steward Observatory, University of Arizona, Tucson, AZ 85721

R. L. DICKMAN: Five College Radio Astronomy Observatory, University of Massachusetts, Amherst, MA 01003

W. H. MCCUTCHEON: Department of Physics, University of British Columbia, Vancouver, BC V6T 2A6, Canada

F. J. VRBA: US Naval Observatory, Flagstaff Station, Flagstaff, AZ 86002